Structure and optical properties of a composite $AsSb-Al_{0.6}Ga_{0.4}As_{0.97}Sb_{0.03}$ metamaterial

© L.A. Snigirev[1], V.I. Ushanov[1], A.A. Ivanov[1], N.A. Bert[1], D.A. Kirilenko[1], M.A. Yagovkina[1], V.V. Preobrazhenskii[2], M.A. Putyato[2], B.P. Semyagin[2], I.A. Kasatkin[3], V.V. Chaldyshev[1,¶]

[1] Ioffe Institute,
194021 St. Petersburg, Russia
[2] Rzhanov Institute of Semiconductor Physics, Siberian Branch, Russian Academy of Sciences,
630090 Novosibirsk, Russia
[3] St. Petersburg State University, St. Petersburg, Russia

¶ E-mail: chald.gvg@mail.ioffe.ru

Received January 19, 2023
Revised February 7, 2023
Accepted February 9, 2023

Epitaxial layers of $Al_xGa_{1-x}As_{1-y}Sb_y$ with an aluminum content $x \sim 60\%$ and antimony content $y \sim 3\%$ were successfully grown by molecular-beam epitaxy at low temperature. A developed system of AsSb nanoinclusions was formed in the semiconductor matrix by subsequent annealing. The extended transparency window of the obtained metamaterial allows us to document the absorption of light near the interband absorption edge of the $Al_xGa_{1-x}As_{1-y}Sb_y$ semiconductor matrix. Parameters of the observed extinction band allow us to attribute the optical absorption to the plasmon resonance in the system of AsSb nanoinclusions.

Keywords: molecular beam epitaxy, x-ray diffraction analysis, transmission electron microscopy, optical properties, plasmon resonance.

DOI: 10.21883/SC.2023.01.55623.4545

1. Introduction

A system of metallic nanoparticles in a semiconductor medium can facilitate the occurrence of the Froelich resonance when the condition of $Re(\varepsilon_m + 2\varepsilon_s) = 0$ is met, where ε_s and ε_m are the dielectric functions of semiconductor and metallic components of the composite material, respectively. Under the conditions of such a resonance, the interaction of light with matter increases [1]. Such an optical medium can exhibit unusual linear and nonlinear properties, which can, for example, be used to create ultrafast saturable absorbers [2]. The integration of such metal-semiconductor metamaterials with semiconductor lasers, LEDs and other optoelectronic components seems promising. Such integration, however, is not feasible for typical plasmonic materials — gold and silver — due to poor compatibility of technologies for obtaining the corresponding nanoparticles and the technology of epitaxial growth of semiconductors. Plasmonic nanoparticles of these materials cannot be obtained in the volume of a semiconductor material, although they can be formed on the surface of grown semiconductor structures using an additional technological process [3,4].

A unique opportunity to form an array of plasmon nanoparticles in the volume of epitaxial layers of GaAs and AlGaAs semiconductors arises when using the technology of low-temperature (LT) molecular beam epitaxy (MBE) [5,6]. The layers of LT-GaAs contain a large amount of super-stoichiometric arsenic, maintaining high crystalline perfection [7,8]. Annealing of such a material after epitaxy activates diffusion processes and leads to the precipitation of excess arsenic with the formation of crystalline semi-metallic nanoinclusions [6,9]. At the same time, the overall crystalline perfection of the material remains high, meeting the standard requirements for semiconductor heterostructures.

The appearance of an array of arsenic nanoinclusions in the GaAs matrix does not significantly change the optical reflection and absorption spectra of the material [6,10]. However, in the case of growing epitaxial layers of solid solutions $GaAs_{1-y}Sb_y$ and $Al_xGa_{1-x}As_{1-y}Sb_y$ ($x \approx 0.3$, $y \approx 0.03$) by LT MBE, the nanoinclusions are highly enriched with antimony [11], and a wide absorption band appears in the optical spectra, which can be associated with the AsSb nanoinclusions system, namely with the Froelich plasmon resonance [12–14]. The absorption coefficient in this band increases with increasing photon energy up to the threshold of interband absorption in the semiconductor matrix. The optical band-to-band absorption in the matrix dominates above this threshold, so that it becomes impossible to observe absorption in nanoparticles against its background. The obvious way to solve this problem is to increase the aluminum content x in the $Al_xGa_{1-x}As_{1-y}Sb_y$ matrix, which should lead to an increase in the band gap of the material and, accordingly, to expand the window of its optical transparency. Such a task is not trivial, since the high concentration of aluminum complicates both the process of epitaxial growth at low temperature and the process of formation of nanoinclusions by annealing structures after growth [15,16].

In this article, we report on the successful growth by LT MBE of $Al_xGa_{1-x}As_{1-y}Sb_y$ epitaxial layers with

nominal values $x = 0.6$, $y = 0.03$, with a thickness of ~ 1 microns, and the formation of a developed system of AsSb nanoinclusions in such layers. We investigated the structure and optical properties of such a metamaterial. We found a strong optical absorption associated with plasmonic nanoparticles in the optical transparency window of the matrix $Al_{0.6}Ga_{0.4}As_{0.97}Sb_{0.03}$ ($\lambda > 600$ nm).

2. Samples and methods

The studied samples were grown using the MBE method on a semi-insulating GaAs substrate with (001) orientation. The condition of the growth surface was controlled *in situ* by reflection high-energy electron diffraction (RHEED). Initially, a 0.2 mm thick GaAs buffer layer was grown on the substrate at a temperature of 580°C at a speed of 1 microns $\cdot$ h^{-1}. Then the gallium flow was interrupted, and the substrate temperature dropped to 200°C. At this temperature, epitaxial layer of $Al_{0.6}Ga_{0.4}As_{0.97}Sb_{0.03}$ was grown. At the initial stages of growth, RHEED demonstrated a diffraction pattern with clear intense reflexes, indicating high crystalline perfection and atomic smoothness of the surface. However, as the epitaxial film grew, diffuse scattering appeared on the RHEED picture and gradually intensified, indicating an increase in surface roughness. We interrupted epitaxy every 100 nm and performed intermediate annealing of the grown epitaxial film at a temperature of 400°C to prevent disruption of epitaxial growth. This procedure allowed for smoothing out the surface relief and eventually grow an epitaxial film with a thickness of 940 nm. The structure was completed with layers of AlAs and GaAs with a thickness of 5 nm each. The absence of additional diffraction features in the diffraction pattern after growth made it possible to assume that the layers did not relax, i.e. they remained in the elastic stressed state.

After growth, the structure was divided into several parts, which were annealed at temperatures of 400–600°C for 15 min in the MBE unit under vapor pressure As.

The methods of X-ray diffraction (XRD), transmission electron microscopy (TEM) and optical spectroscopy (OS) were used to characterize the samples.

X-ray diffraction studies were conducted using the equipment of the resource center of the St. Petersburg State University Research Park, XRD Center. A high-resolution diffractometer D8-DISCOVER from Bruker with an X-ray tube with $\lambda = 1.5406$ A was used. X-ray diffraction curves were recorded near the 004 reflex of the GaAs substrate. Experimental curves were modeled using the software package LEPTOS.

Studies of optical reflection, transmission and absorption were carried out at room temperature at normal light incidence in the ranges of 400–1000 and 900–1600 nm using OceanOptics QE65Pro and NIRQuest-512 spectrometers, respectively. The OceanOptics SpectraSuite software package was used for recording and primary processing of spectra. The spectrum of the light absorption coefficient was determined by measuring the reflection and transmission spectra in a constant geometry. Since the GaAs substrate is opaque in the wavelength range $\lambda < 870$ nm, for optical measurements its central region with a diameter of 1 mm was removed by selective chemical etching.

Structural studies were carried out using TEM with the equipment of the Center for Collective Use („Materials science and characterization in advanced technologies“ at Ioffe Institute) to identify AsSb nanoparticles in the AlGaAs matrix, analyze their sizes and concentrations. Samples for TEM were made in (110) cross section according to the standard procedure with preliminary thinning by mechanical treatment and finishing ion sputtering. The studies were conducted using an electron microscope JEM-2100F (JEOL, Japan) with an accelerating voltage of 200 kV in the TEM, high-angle annular dark-field scanning transmission electron microscopy (STEM-HAADF) and energy dispersive X-ray spectroscopy (EDXS) modes.

3. Results and discussion

Figure 1 shows the experimental and calculated X-ray diffraction curves of the $Al_{0.6}Ga_{0.4}As_{0.97}Sb_{0.03}$ sample annealed at 600°C. The left peak in the figure corresponds to the 004 Bragg reflex from the epitaxial layer, and the right peak is reflection from the GaAs substrate. A good quantitative match of the calculated and experimental curves allows determination of the lattice period of the epitaxial layer in the direction of growth. Its value turned out to be 0.5697 nm. The difference between the lattice parameter of the epitaxial layer and the lattice parameter of the GaAs substrate depends on both the concentration of aluminum x and the concentration of antimony y. XRD measurements alone are not sufficient to determine both of these values.

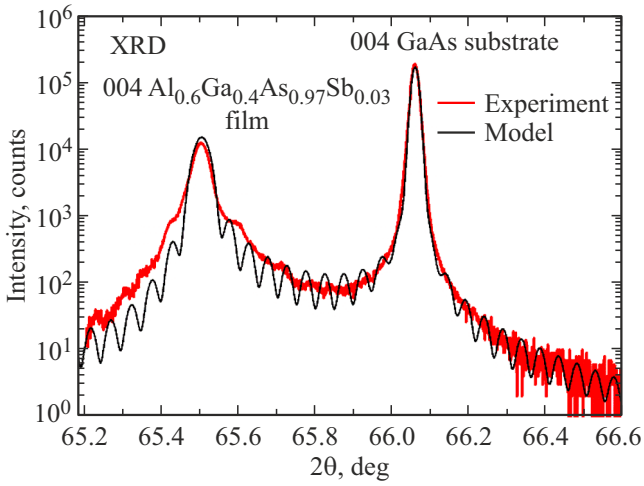

Figure 1. Experimental (red) and calculated (black) X-ray diffraction curves for AsSb–$Al_{0.6}Ga_{0.4}As_{0.97}Sb_{0.03}$ metamaterial grown on GaAs substrate.

Figure 2 shows a bright-field electron microscopic image of a (110) cross-section of the AsSb–$Al_{0.6}Ga_{0.4}As_{0.97}Sb_{0.03}$ annealed at 600°C, formed in two-beam conditions with an active diffraction vector $g = 220$. The total thickness of the sample is 940 nm. AsSb nanoinclusions, due to the higher mass density, create contrast in the image in the form of small dark spots scattered over the volume of the epitaxial film.

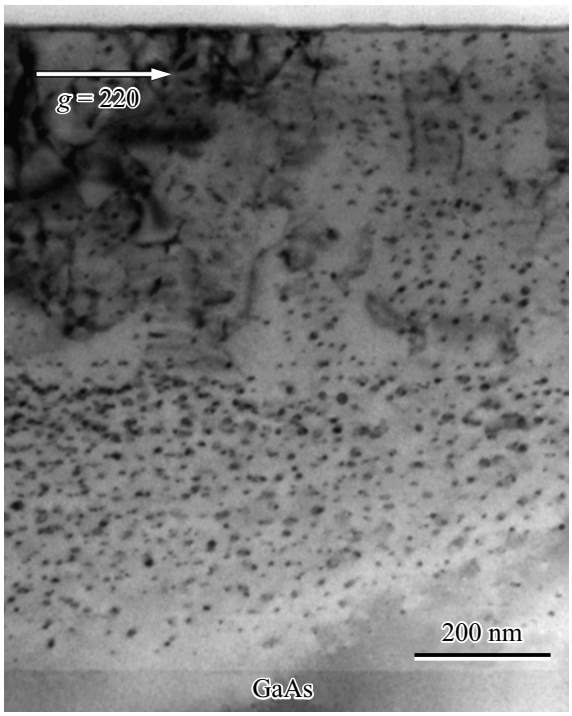

Figure 2. Bright-field electron microscopic image under bi-beam conditions ($g = 220$) of the (110) cross-section of the AsSb–$Al_{0.6}Ga_{0.4}As_{0.97}Sb_{0.03}$ sample after annealing at 600°C.

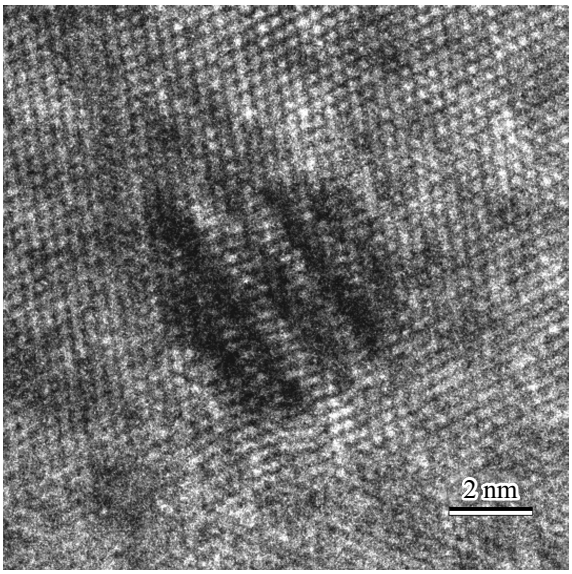

Figure 3. Electron microscopic image of AsSb nanoinclusions in the $Al_{0.6}Ga_{0.4}As_{0.97}Sb_{0.03}$ matrix in high resolution mode.

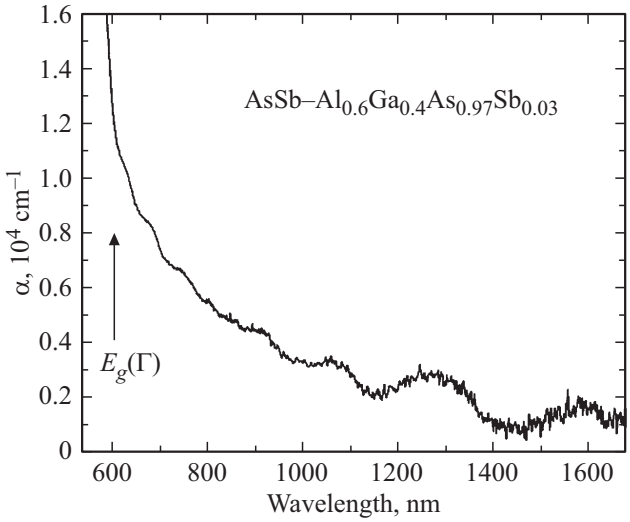

Figure 4. Optical extinction spectrum in the metamaterial layer AsSb–$Al_{0.6}Ga_{0.4}As_{0.97}Sb_{0.03}$. $T = 300$ K.

A typical high-resolution electron microscopic image of one of the AsSb nanoinclusions is shown in Fig. 3. The atomic planes (111) and $(11\bar{1})$ of the matrix $Al_{0.6}Ga_{0.4}As_{0.97}Sb_{0.03}$ are well resolved in the image. The presence of a crystalline nano-inclusion in the matrix volume causes moire fringes at its location resulting from the interference of Bragg reflections from the atomic planes in $Al_{0.6}Ga_{0.4}As_{0.97}Sb_{0.03}$ and AsSb with close interplanar distances. The diameter of the nanoinclusion shown in Fig. 3 is ~ 6 nm.

The analysis of electron microscopic images acquired using STEM-HAADF mode together with EDXS showed a high (estimated 50%) antimony content in nanoinclusions with a small (nominally 3%) content of this element in the matrix $Al_xGa_{1-x}As_{1-y}Sb_y$.

Statistical processing of TEM images allowed for determining the main parameters of the AsSb nanoinclusion system. The average concentration of nanoinclusions was $2 \cdot 10^{16}$ cm^{-3}, their average diameter is 6 nm. The average particle volume was 196 nm^3, so that nanoinclusions occupy $\sim 0.4\%$ of the total volume of the epitaxial film.

Figure 4 shows the optical extinction spectrum in the metamaterial layer AsSb–$Al_{0.6}Ga_{0.4}As_{0.97}Sb_{0.03}$ at 300 K. The light extinction coefficient was calculated using the Bouguer–Lambert–Beer law based on experimental data on optical reflection and transmission according to the formula $\alpha = -\ln \frac{T}{(1-R)}/d$, where d — epitaxial film thickness, R and T — light reflection and transmission coefficients.

A sharp increase of the light absorption coefficient is seen in the region of short wavelengths due to direct interband transitions in the $Al_xGa_{1-x}As_{1-y}Sb_y$ semiconductor matrix. The band gap E_g of a solid solution at the point Γ of the Brillouin zone can be determined from the reflection spectrum. The data on $E_g(\Gamma)$ and the lattice parameter determined from the XRD curves as described above allow

an independent determination of the values of x and y in the chemical formula of the $Al_xGa_{1-x}As_{1-y}Sb_y$ solid solution [11]. These values turned out to be equal to $x = 0.553$, $y = 0.037$, which with a reasonable accuracy corresponds to nominal values $x = 0.6$ and $y = 0.03$ used as a reference for epitaxial growth conditions. It should be noted that the kinetics and thermodynamics of epitaxial growth of layers of this composition at low temperature have not been studied before.

Figure 4 shows that the extinction spectrum is modulated by oscillations, the amplitude of which increases with increasing wavelength. The central region of the GaAs substrate was removed to measure the optical properties of the metamaterial in the entire transparency window of the matrix $Al_{0.6}Ga_{0.4}As_{0.97}Sb_{0.03}$. Very large dielectric contrast at the air-epitaxial film interfaces in the measured optical reflection $R(\lambda)$ and transmission $T(\lambda)$ spectra resulted in the Fabry–Perot oscillations. The magnitude of the oscillations depends on the absorption of light in the $Al_{0.6}Ga_{0.4}As_{0.97}Sb_{0.03}$ layer, — the amplitude of the oscillations is relatively large in the area of small absorption, while the oscillations are hardly noticeable in the area of stronger absorption which is well illustrated by Fig. 4. The presence of a surface relief at the bottom of the chemical etching pit violates the coherence of the incident and reflected light streams, but the experimental conditions used prevent the complete removal of oscillations in the spectrum $\alpha(\lambda)$ when measuring films with a removed substrate. A detailed analysis of the relevant phenomena is outside the scope of this work.

Experimental data in Fig. 4 indicate that light is absorbed in the metamaterial in the transparency region of the matrix ($\lambda > 600$ nm) and the absorption coefficient slowly decreases from $1 \cdot 10^4$ cm^{-1} at $\lambda = 650$ nm to values close to zero at $\lambda = 1500$ nm. Such absorption cannot be related to the Urbach tail or fluctuations in the band gap in solid solution. The characteristic energy scale for these mechanisms is orders of magnitude smaller than the observed one. The observed absorption cannot be related to the effects of strong doping, since the samples were not doped specifically, and the residual concentration of impurities in III–V materials grown by the MBE method is very small. This absorption cannot be associated with intrinsic point defects, since in the annealing process such defects form a system of nanoinclusions, and their concentration becomes equilibrium, i.e. low [5,6,8]. This process is reliably documented by XRD and TEM methods. Optical radiation scattered at various angles at the rough boundary after etching also cannot make a significant contribution to extinction in the considered wavelength range. This, in particular, is confirmed by the fact that characteristic absorption is also observed in similar metamaterials that have not been chemically etched [13].

A wide band of light extinction in the transparency region of the matrix can be associated with plasmon resonance in a system of metal nanoparticles embedded in a semiconductor matrix, if the Froelich resonance condition $Re(\varepsilon_m + 2\varepsilon_s) = 0$ is met in this wavelength region [10]. Numerous optical studies (see, for example, [5–8,10]) have shown that the Froelich resonance in the transparency region of the matrix does not manifest itself for $As-Al_xGa_{1-x}As$ metamaterials. However, in the case of $AsSb-Al_xGa_{1-x}As_{1-y}Sb_y$ metamaterials in which nanoinclusions contain a large concentration of antimony [11], the corresponding resonant light absorption was detected [13,14]. The absorption spectrum shown in Fig. 4 agrees well with the data of [13,14]. At the same time, the plasmon absorption can be observed in a wider range of wavelengths in this work.

The results of structural studies obtained in this work allow us making a conclusion about the strong segregation of antimony in nanoinclusions formed in the studied metamaterial based on $Al_{0.6}Ga_{0.4}As_{0.97}Sb_{0.03}$. It is not possible to quantify the exact antimony concentration in nanoinclusions immersed in the matrix, however, the enrichment turned out to be strong enough for reliable detection using EDXS method [17] which is ensured with antimony concentrations of 50% or more. The concentration of Sb in nanoinclusions exceeded 90% in the previously studied metamaterial based on $Al_{0.3}Ga_{0.7}As_{0.97}Sb_{0.03}$. It can be estimated that the dielectric properties of nanoinclusions are close to the properties of antimony based on the similarity of structural parameters and optical properties in the spectral transparency window of these related metamaterials. Using data on the permittivity of antimony [18], it can be assumed that the Froelich plasmon resonance is realized with a maximum in the wavelength range of 500–600 nm, i.e., near the edge of the interband absorption in the studied $Al_{0.6}Ga_{0.4}As_{0.97}Sb_{0.03}$ solid solution. In this case, the full width at half maximum of the resonance should be 1.5–2 eV. For optical absorption coefficient of the plasmon nanoparticle system to reach $\sim 1 \cdot 10^4$ cm^{-1} at $\lambda = 650$ nm their volume fraction in the metamaterial should be $f = 0.4–0.5\%$. This value is quantitatively consistent with the value of f determined experimentally using the TEM method ($\sim 0.4\%$).

Thus, the plasmonic nature of the observed resonance ensures a sufficiently effective absorption of light despite the very small fraction of the volume occupied by AsSb nanoparticles in the $Al_{0.6}Ga_{0.4}As_{0.97}Sb_{0.03}$ epitaxial layer. At the same time, the large spectral resonance width indicates that plasmon excitation in such nanoparticles is characterized by an ultrashort relaxation time of the order of several femtoseconds. Such a metamaterial may be promising for use in optical and optoelectronic elements, in which the recovery time is a key parameter. It should be noted that the used technology of low-temperature epitaxy is fully compatible with the standard MBE technology used for the production of semiconductor lasers, LEDs and other devices. At the same time, the use of growth interruptions and intermediate annealing can provide layers with a thickness sufficient to solve many applied problems.

4. Conclusion

The conducted studies have shown that, despite the significant difficulties associated with the kinetics of low-temperature MBE of $Al_xGa_{1-x}As_{1-y}Sb_y$ solid solutions with an aluminum content of $x \approx 0.6$, epitaxial films of such a material with a thickness of up to 1 microns can be successfully obtained. Growth interruptions and intermediate annealing can be used to preserve high crystalline perfection of the grown layers. High-temperature postgrowth annealing leads to the formation of a developed system of AsSb nanoinclusions in the $Al_{0.6}Ga_{0.4}As_{0.97}Sb_{0.03}$ semiconductor matrix. As a result of annealing at 600°C for 15 min, the average size of the produced nanoparticles is 6 nm, their average volume is close to 200 nm^3. At a concentration of nanoparticles $2 \cdot 10^{16}$ cm^{-3}, the volume of metamaterial occupied by them is $\sim 0.4\%$. Such a system of antimony-enriched plasmon nanoparticles embedded in the $Al_{0.6}Ga_{0.4}As_{0.97}Sb_{0.03}$ matrix ensures light absorption in a broad spectral region near the threshold of interband absorption of the semiconductor matrix. The corresponding optical absorption coefficient reaches $1 \cdot 10^4$ cm^{-1}.

Funding

The study was supported by a grant from the Russian Science Foundation No. 22-22-20105 (https://rscf.ru/project/22-22-20105/) and a grant from the St. Petersburg Science Foundation in accordance with agreement No. 2022/25 dated April 14.

Conflict of interest

The authors declare that they have no conflict of interest.

References

[1] S.A. Maier. *Plasmonics: Fundamentals and Applications* (N.Y., Springer, 2007).
[2] D. Zhao, Y. Liu, J. Qiu, X. Liu. Adv. Photonics Res., **2**, 2100003 (2021).
[3] N.A. Toropov, I.A. Gladskikh, P.V. Gladskikh, A.N. Kosarev, V.V. Preobrazhenskii, M.A. Putyato, B.R. Semyagin, V.V. Chaldyshev, T.A. Vartanyan. J. Opt. Technol., **84**, 459 (2017).
[4] A.N. Kosarev, V.V. Chaldyshev, A.A. Kondikov, T.A. Vartanyan, N.A. Toropov, I.A. Gladskikh, P.V. Gladskikh, I. Akimov, M. Bayer, V.V. Preobrazhensky, M.A. Putyato, B.R. Semyagin. Opt. Spectrosc., **126**, 492 (2019).
[5] M.R. Melloch, J.M. Woodall, E.S. Harmon, N. Otsuka, F.H. Pollak, D.D. Nolte, R.M. Feenstra, M.A. Lutz. Ann. Rev. Mater. Sci., **25**, 547 (1995).
[6] N.A. Bert, A.I. Veinger, M.D. Vilisova, S.I. Goloshchapov, I.V. Ivonin, S.V. Kozyrev, A.E. Kunitsyn, L.G. Lavrent'eva, D.I. Lubyshev, V.V. Preobrazhenskii, B.R. Semyagin, V.V. Tret'yakov, V.V. Chaldyshev, M.P. Yakubenya. Phys. Solid State, **35**, 1289 (1993).
[7] X. Liu, A. Prasad, J. Nishio, E.R. Weber, Z. Liliental-Weber, W. Walukiewicz. Appl. Phys. Lett., **67**, 279 (1995).
[8] L.G. Lavrent'eva, M.D. Vilisova, V.V. Preobrazhenskii, V.V. Chaldyshev. Crystallogr. Rep., **47**, S118 (2002).
[9] A.C. Warren, J.M. Woodall, J.L. Freeouf, D. Grischkowsky, D.T. McInturff, M.R. Melloch, N. Otsuka. Appl. Phys. Lett., **57**, 1331 (1990).
[10] D.D. Nolte. J. Appl. Phys., **76**, 3740 (1994).
[11] N.A. Bert, V.V. Chaldyshev, N.A. Cherkashin, V.N. Nevedomskii, V.V. Preobrazhenskii, M.A. Putyato, B.R. Semyagin, V.I. Ushanov, M.A. Yagovkina. J. Appl. Phys., **125**, 145106 (2019).
[12] P.V. Lukin, V.V. Chaldyshev, V.V. Preobrazhensky, M.A. Putyato, B.R. Semyagin. Semiconductors, **46**, 1291 (2012).
[13] V.I. Ushanov, V.V. Chaldyshev, N.D. Ilyinskaya, N.M. Lebedeva, M.A. Yagovkina, V.V. Preobrazhensky, M.A. Putyato, B.R. Semyagin. Phys. Solid State, **56**, 1952 (2014).
[14] V.I. Ushanov, V.V. Chaldyshev, N.A. Bert, V.N. Unknown, N.D. Ilyinskaya, N.M. Lebedeva, V.V. Preobrazhensky, M.A. Putyato, B.R. Semyagin. Semiconductors, **49**, 1587 (2015).
[15] M.N. Chang, K.C. Hsieh, T.-E. Nee, J.-I. Chyi. J. Appl. Phys., **86**, 2442 (1999).
[16] N. Cherkashin, A. Claverie, C. Bonafos, V.V. Chaldyshev, N.A. Bert, V.V. Preobrazhenskii, M.A. Putyato, B.R. Semyagin, P. Werner. J. Appl. Phys., **102**, 023520 (2007).
[17] N. Bert, V. Ushanov, L. Snigirev, D. Kirilenko, V. Ulin, M. Yagovkina, V. Preobrazhenskii, M. Putyato, B. Semyagin, I. Kasatkin, V. Chaldyshev. Materials, **15**, 7597 (2022).
[18] M. Cardona, D.L. Greenaway. Phys. Rev. A, **133**, 1685 (1964).

Translated by A.Akhtyamov